

Realization of a low threshold multiwavelength Brillouin/erbium fiber laser by optimizing the reflected power

A. W. Al-Alimi^{1,2*}, A. F. Abas^{1,2}, M. A. Mahdi^{1,2}, M. H. Al-Mansoori³, and M. Mokhtar^{1,2}

¹Wireless and Photonic Networks Research Centre, Engineering and Technology Complex,
Universiti Putra Malaysia, 43400 Serdang, Selangor, Malaysia

²Photonics and Fiber Optic Systems Laboratory, Department of Computer and Communication Systems Engineering,
Universiti Putra Malaysia, 43400 Serdang, Selangor, Malaysia

³Faculty of Engineering, Sohar University, P. O Box 44, Sohar P. C. 311, Oman

*Corresponding author: mogni.66@yahoo.com

Received April 30, 2012; accepted July 10, 2012; posted online October 16, 2012

A multiwavelength Brillouin/erbium fiber laser (BEFL) with low threshold power is realized. A low threshold power of 3 mW and a wide tuning range of 18 nm can be achieved by controlling the reflected power in the nonlinear optical loop mirror (NOLM). Up to 24 lines with a wavelength spacing of 0.086 nm are generated at the Brillouin pump and at the 1 480-nm pump with -0.5 dBm (0.9 mW) and 25 mW of power, respectively.

OCIS codes: 140.3510, 290.5900, 060.2410.

doi: 10.3788/COL201210.121401.

The multi-wavelength laser sources have been used in many applications, such as in dense wavelength division multiplexing (DWDM) systems, optical fiber sensors, and microwave photonics^[1,2]. By offering cost-saving solutions, the erbium-doped fiber laser (EDFL) has attracted much interest in its use as a multi-wavelength laser source. However, the homogeneous linewidth of the gain medium in EDFLs should be reduced, and the mode competition between adjacent laser signals should be suppressed. Several techniques have been proposed to solve this problem, such as cooling down the EDF to liquid nitrogen temperature^[3], using frequency-shifted feedback^[4], and optimizing the cavity loss^[5,6]. Other multiwavelength sources that utilize different nonlinear effects, such as four-wave mixing (FWM)^[7,8], nonlinear polarization rotation (NPR)^[9], stimulated Brillouin scattering (SBS)^[10], and stimulated Raman scattering (SRS)^[11] were previously reported. The inadequate Brillouin gain in the single mode fiber requires another gain medium to compensate the cavity loss and to improve the laser operation efficiency. This concept was successfully demonstrated by Cowle and Stepanov^[12]. The combination of the SBS effect and the EDF in the same laser cavity creates a Brillouin/erbium fiber laser (BEFL). Different BEFL structures have been proposed to generate multiple wavelengths when achieving low threshold values and low pump power per channel are both very important. The pre-amplification technique in a linear cavity^[13–18] is widely used to reduce the SBS threshold and to enhance the performance of the BEFL. The reverse-S-shaped section was used as another method to reduce the threshold power, in which the Brillouin Stokes (BS) signals couple back into the laser cavity^[19]. However, in this structure, the use of many optical components requires a high threshold power. When the reverse-S-shaped fiber section was replaced by a broad-

band, partially reflecting fiber Bragg grating (FBG), the threshold power was improved^[20]. The transmission and the reflection power intensity of the nonlinear optical loop mirror (NOLM) have been investigated by Doran *et al.*^[21]. The rapid auto-switching ability of the NOLM makes it a valuable technique in optical signal processing applications, which include pulse shaping^[22], amplitude equalizing^[23], and self-switching^[24]. More studies^[25,26] have recently exploited the effect of the NOLM as an effective component to improve the BEFL performance.

In this letter, multiwavelength BEFL was experimentally demonstrated. Beside the double pass amplification method, the power intensity levels in the NOLM was optimized by the proper adjustment of the output coupling ratio of the variable optical coupler (VOC) to achieve low threshold power. A low threshold power of about 3 mW at a Brillouin pump (BP) power of 0 dBm was reported.

The experimental setup of the proposed tunable BEFL is shown in Fig. 1. The linear cavity structure simply consists of two circulators (C1 and C2), one VOC, a 1 480-nm wavelength selective coupler (WSC), and 10-m-long EDF with an absorption coefficient of 5.6 dB/m at 1 531 nm. The wavelength selective coupler (WSC) was used to combine the 1 480-nm pump power and the oscillating signals. C1 was used as input and output port, whereas C2 was used to form a fiber loop mirror (FLM) in which the laser guided back to the cavity. The BP power and wavelength were provided by an external-cavity tunable laser source (TLS) with a maximum power of 8 dBm and 200-kHz line width. The TLS can be tuned over a tuning range of 100 nm (from 1 520 to 1 620 nm). An optical spectrum analyzer (OSA) with 0.01-nm resolution was connected to port 3 of C1 to monitor the BEFL output.

The NOLM was formed by splicing a 3-km standard

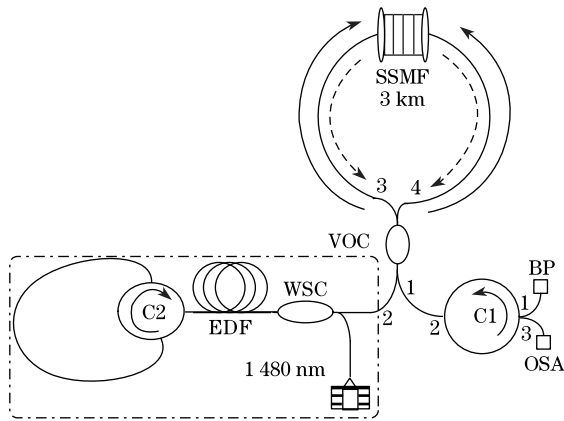


Fig. 1. Experimental setup of the BEFL.

single mode fiber (SSMF), used as the Brillouin gain medium, between port 3 and port 4 of the VOC, as shown in Fig. 1. When the power was injected through port 1 of the VOC, it is split into two counter-propagating signals (P_1 and P_2). Both signals are propagated inside the SSMF in opposite directions. The power intensity of two signals can be calculated as^[25]

$$P_1 = K^{(1/2)} P_{in} \cdot e^{-\frac{jK|P_{in}|^2 2\pi n_2 L}{\lambda}},$$

$$P_2 = j(1 - K)^{1/2} P_{in} \cdot e^{-\frac{j(1-K)|P_{in}|^2 2\pi n_2 L}{\lambda}},$$

where P_{in} is the input power, K is the splitting ratio of variable optical coupler, L is the loop length, n_2 is the refractive index coefficient, and λ is the operating wavelength. Due to the self phase modulation (SPM), the phase velocity of each signal depends on its respective intensity; therefore, a non linear phase shift between the counterclockwise (CCW) and clockwise (CW) signals is induced. The phase shift difference between the two counter-propagation signals during a round trip can be calculated by^[21]

$$\Delta\phi = P_{in} L (1 - 2k) \frac{2\pi n_2}{\lambda}. \quad (1)$$

The two signals are combined interferometrically at the VOC and denoted as the transmitted (P_t) and reflected (P_r) power of the NOLM. These signals can be calculated by^[21]

$$P_t = P_{in} \{1 - 2K(1 - K)(1 + \cos[(1 - 2K)\Delta\phi])\}, \quad (2)$$

$$P_r = P_{in} \{2K(1 - K)(1 + \cos[(1 - 2K)\Delta\phi])\}. \quad (3)$$

From Eqs. (1)–(3), beside the P_{in} , L , λ , and n_2 the transmitted and reflected power of the NOLM depends on the splitting ratio of the VOC, which is represented by the parameter K ^[21]. This implies that the transmitted and reflected power of the NOLM can be controlled by adjusting the output coupling ratio.

Figure 2 depicts the transmitted and reflected power of the NOLM as a function of the output coupling ratio. The tunable laser source was fixed at 1 550 nm with a 7.5-dBm output power. The EDF and WSC were removed from the setup, and the laser power was injected

into port 2 of the VOC through port 1 of the C2. The transmitted and reflected powers were measured at port 1 of the VOC and port 3 of the C2, respectively. At an output coupling ratio of 39%, only a small amount of the power was transmitted, whereas the majority was reflected back. Therefore, the NOLM can act as a high reflective mirror, in which most of the laser power reflects back to the cavity. By measuring the power of the CCW and CW signals at the said ratio, the two signals were found to approximately equal amplitudes. Other non-symmetric ratio of the VOC can also cause the NOLM to act as a weak reflective mirror, such as 58%, 75%, and 83%. To achieve a low threshold power, the output coupling ratio of 39% was observed to be the optimum ratio. In addition, the double pass amplification technique causes the Brillouin Stokes lines to be amplified twice, which also contributes towards decreasing the threshold power^[27].

In general, the laser can be formed between the VOC and the C2 when the total Brillouin and erbium gains are equal to the cavity loss. The first-order BS signal, which is down-shifted by 0.086 nm from the Brillouin pump wavelength, propagates in the opposite direction of the injected BP, as shown in Fig. 1. When the Brillouin threshold condition is satisfied, the first-order BS signal serves as a Brillouin pump signal to create the second-order BS signal. This process continues until the power of the next higher-order BS signal becomes too weak to satisfy the Brillouin threshold condition. At the steady-state condition, a stable laser can be produced at port 3 of the C1, which originates from the reflected BP and its Brillouin Stokes signals.

One of the parameters that determine the laser efficiency is the threshold power of the resonator. In any laser system, a low threshold power is critical and desirable. In a BEFL, at a fixed BP power, the threshold power that is required to produce the first Stokes line can be determined by the amount of pump power injected into the EDF. In this measurement, the 1 480-nm power was varied, whereas the BP power was fixed at 0 dBm. The change of the output coupling ratio of the VOC was observed to cause a change in the EDF peak gain region. Therefore, the BP wavelength was tuned to EDF peak gain region. Figure 3 shows the effect of the output coupling ratio on the threshold power. When the output coupling ratio was tuned up to 39%, the laser output power at port 1 was reduced. This implies that most of the laser power was returned back to the cavity.

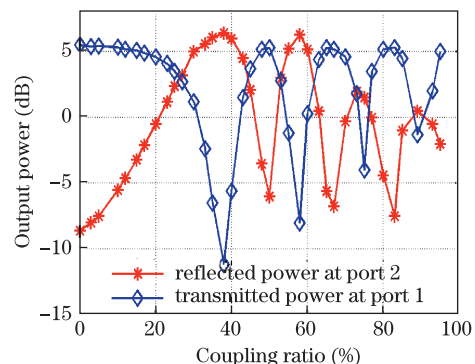


Fig. 2. Transmitted and reflected power of the nonlinear fiber loop mirror as a function of the output coupling ratio.

Therefore, the pump power required to amplify the injected BP signal and to satisfy the threshold condition was gradually reduced as the coupling ratio was gradually increased to 39%. On the other hand, due to tap more power from the cavity when the output coupling ratio was varied from 39% to 49%, the threshold power was increased. A low threshold power can also be obtained with the coupling ratios of 58%, 75%, and 83%.

Table 1 lists the threshold power and Brillouin pump power reported in previous studies. It can be concluded that a high pump power was required to amplify the BP power such that it would reach the SBS threshold, for example, 3 dBm in Refs. [20] and [28] or 6 dBm in Ref. [29]. However, in this experiment, a low threshold power of 3 mW was obtained at a low BP power of 0 dBm (1 mW). Therefore, this configuration reduced the pump power required by 57%, 70%, and 40% as compared with the results presented in Refs. [20], [28], and [29], respectively. In Ref. [30], the same threshold power was obtained, thus a 0% reduction was achieved. However, in that setup, 2 dBm (1.6 mW) of Brillouin pump power must be injected into the cavity, which is higher than the one achieved in this letter.

Table 1. Threshold Reduction Obtained by the Present Setup Relative to the Previous Work

Ref.	BP (dBm)	Threshold (mW)	Threshold Reduction Relative to the Present Study
[20]	3.0	7.0	57%
[28]	3.0	10.0	70%
[29]	6.0	5.0	40%
[30]	2.0	3.0	0%
Present Study	0.0	3.0	–

The effect of the BP power on the threshold power has also been investigated. In general, the threshold power was reduced from 3 to 2 mW as the BP power was increased from -1 to 6 dBm. Therefore, the threshold power obtained in this letter can be considered as the lowest value that has ever been reported. This low threshold is attributed to the double-pass amplification, and the efficient circulation of the laser power inside the cavity.

Figure 4 depicts the tuning range and the corresponding number of output channels against different output coupling ratios. The pump power of 1480 nm and the BP pump power were fixed at 25 mW and 4 dBm, respectively. The self-lasing cavity mode region of the EDFL varies as the output coupling ratio was tuned. Therefore, to obtain the maximum number of channels, the wavelength of BP is tuned to the EDF peak gain region. Figure 4 shows that the number of wavelengths and the tuning range strongly depend on the optimization of the transmitted and reflected power of the NOLM, which is controlled by adjusting the output coupling ratio of the VOC. A total of 14 wavelengths and a low tuning range of 3 nm were obtained when the output coupling ratio of the VOC was set to 39%, in which most of laser power is circulated inside the cavity. However, at the expense of low wavelengths count, a wider tuning range of 18 nm was obtained by adjusting the output coupling ratio to either 0%, 10%, or 90% because more power can

reach the output port, which consequently leads to the reduced mode competition between the Stokes lines and the self-lasing cavity modes.

Figure 5 depicts the effects of the 1 480-nm pump power on the number of BS signals generated. The output coupling ratio was fixed at 39%, the BP power at 0 dBm, and the BP wavelength at 1 562.6 nm, which is equivalent to the first edge of the lasing wavelength of the free-running cavity modes. The number of Stokes signals can be maximized by optimizing the pump power. Therefore, the 1 480-nm pump power was varied from 10 to 30 mW. As the pump power was increased, the EDF gain was improved. This consequently increased the number of BS signals, as depicted in Figs. 5(a)–(c). Figure 5(c) clearly shows that the highest number of Stokes signals was obtained with a pump power of 25 mW. At pump power of 30 mW, the increased pump power that was injected to the EDF caused the self-lasing cavity modes to gain more energy than the higher-order Stokes lines. Thus, the power of the higher-order Stokes signals becomes insufficient to suppress the free-running cavity modes. For this reason, in addition to the BS signals, the free-running cavity modes appeared, with a peak power of approximately -20 dBm, which is equal to the highest-order power of the Stokes signals, as shown in Fig. 5(d). To obtain large number of stable channels, the 1 480-nm pump power, the BP power, and the BP wavelength should all be optimized. In the optimization process, the BP wavelength was fixed at 1 562.9 nm where the self-lasing cavity modes were totally suppressed. The BP power was varied from -1 to 6 dBm in 0.5-dBm steps while the 1 480-nm pump power was fixed at 25 mW. The large number of wavelengths of the BEFL was obtained when the BP power was -0.5 dBm. Figure 6 shows the maximum number

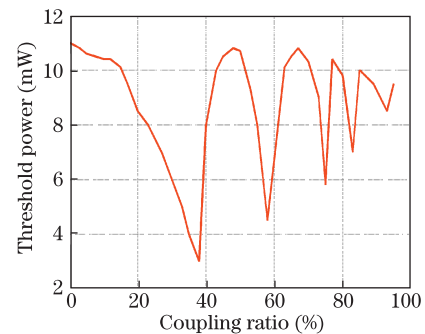


Fig. 3. Threshold power as a function of the coupling ratio.

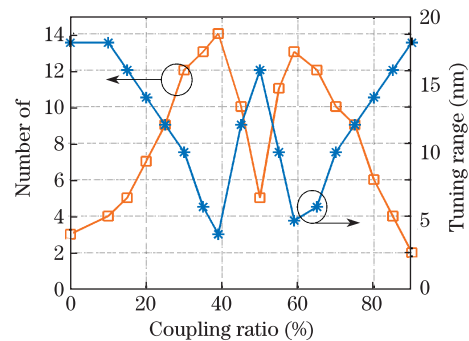


Fig. 4. Effect of the output coupling ratio on the output channels number and the tuning range at pump power of 25 mW and at Brillouin pump power of 4 dBm.

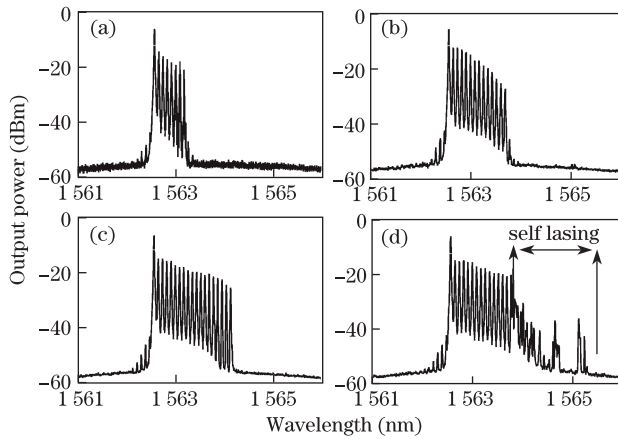


Fig. 5. Output spectra of the proposed laser at 39% for a fixed Brillouin pump power of 0 dBm at a fixed wavelength of 1562.6 nm, and at different levels of 1480-nm pump power: (a) 10 mW, (b) 15 mW, (c) 25 mW, and (d) 30 mW.

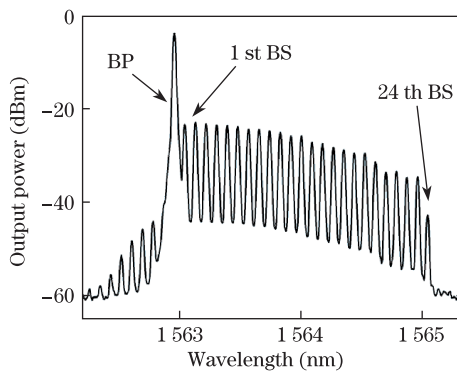


Fig. 6. Output spectrum of the proposed laser at a Brillouin pump power of -0.5 dBm and at a 1480-nm pump power of 25 mW.

of wavelengths obtained from the laser structure at the optimum conditions of the BP and the pump power.

In conclusion, the realization of multiwavelength Brillouin/erbium fiber laser with a low threshold power of 3 mW is successfully demonstrated. The low threshold power is achieved by optimizing the reflected power to the cavity. The optimization of reflected power and the wavelength and power of the Brillouin pump, as well as the power of the 1480-nm pump laser, are essential to achieve the maximum possible number of Stokes lines. Up to 24 channels are obtained at pump power of 25 mW, BP power of -0.5 dBm, and BP wavelength of 1562.9 nm. The gain competition between the self-lasing cavity modes and BS lines can be reduced by reducing the power that is reflected to the cavity. A wide tuning range of 18 nm can be achieved with output coupling ratios of either 0%, 10%, or 90%. This very useful finding can become a part of the solution to the high-threshold issues in the design of multiwavelength fiber lasers.

References

1. A. Bellemare, M. Karasek, M. Rochette, S. LaRochelle, and M. Tetu, *J. Lightwave Technol.* **18**, 825 (2000).
2. G. Shen, X. Zhang, H. Chi, and X. Jin, *Progress in Electromagnetics Research* **80**, 307 (2008).
3. S. Yamashita and K. Hotata, *Electron. Lett.* **32**, 1298 (1996).
4. K. Zhou, D. Zhou, F. Dong, and N. Q. Ngo, *Opt. Lett.* **28**, 893 (2003).
5. A. W. Al-Alimi, M. H. Al-Mansoori, A. F. Abas, M. A. Mahdi, M. Ajiya, and F. R. Mahamd Adikan, *Laser Phys.* **20**, 2001 (2010).
6. A. W. Al-Alimi, M. H. Al-Mansoori, A. F. Abas, M. A. Mahdi, F. R. M. Adikan, and M. Ajiya, *Laser Phys.* **19**, 1850 (2009).
7. H. Ahmad, R. Parvizi, K. Dimyati, M. R. Tamjis, and S. W. Harun, *Laser Phys.* **20**, 1414 (2010).
8. X. Yang, X. Dong, S. Zhang, F. Lu, X. Zhou, and C. Lu, *IEEE Photon. Technol. Lett.* **17**, 2538 (2005).
9. Q. Xu and X. Ma, *Laser Phys.* **21**, 1092 (2011).
10. R. Parvizi, N. M. Ali, S. W. Harun, M. Moghavvemi, H. Arof, and H. Ahmad, *Laser Phys.* **21**, 205 (2011).
11. Y. G. Han, J. H. Lee, S. B. Lee, L. Poti, and A. Bogoni, *J. Lightwave Technol.* **25**, 2219 (2007).
12. G. J. Cowle and D. Y. Stepanov, *Opt. Lett.* **21**, 1250 (1996).
13. M. H. Al-Mansoori, M. A. Mahdi, and A. K. Zamzuri, *Laser Phys. Lett.* **5**, 139 (2008).
14. M. N. M. Nasir, Z. Yusoff, M. H. Al-Mansoori, H. A. Abdul Rashid, and P. K. Choudhury, *Opt. Express* **17**, 12829 (2009).
15. S. Shahi, S. W. Harun, N. S. Shahabuddin, M. R. Shirazi, and H. Ahmada, *Opt. Laser Technol.* **41**, 198 (2009).
16. M. H. Al-Mansoori and M. A. Mahdi, *Appl. Opt.* **48**, 3424 (2009).
17. M. H. Al-Mansoori, M. Kamil Abd-Rahman, F. R. Mahamad Adikan, and M. A. Mahdi, *Opt. Express* **13**, 3471 (2005).
18. Z. Abd Rahman, M. H. Al-Mansoori, S. Hitam, A. F. Abas, M. H. Abu Bakar, and M. A. Mahdi, *Laser Phys.* **19**, 2110 (2009).
19. N. M. Samsuri, A. K. Zamzuri, M. H. Al-Mansoori, A. Ahmad, and M. A. Mahdi, *Opt. Express* **16**, 16475 (2008).
20. M. Johari, A. Adamiat, N. Shahabuddin, M. Nasir, Z. Yusoff, H. Abdul Rashid, M. Al-Mansoori, and P. Choudhury, *J. Opt. Soc. Am. B* **26**, 1675 (2009).
21. N. J. Doran and D. Wood, *Opt. Lett.* **13**, 56 (1988).
22. J. Lee, Y. M. Chang, and J. H. Lee, *Opt. Lett.* **36**, 4227 (2011).
23. X. Feng, H. Tam, H. Liu, and P. K. A. Wai, *Opt. Commun.* **268**, 278 (2006).
24. W.-H. Cao and P. K. A. Wai, *Opt. Commun.* **245**, 177 (2005).
25. M. H. Al-Mansoori and M. A. Mahdi, *J. Lightwave Technol.* **27**, 5038 (2009).
26. M. H. Al-Mansoori and M. A. Mahdi, *Opt. Express* **19**, 23981 (2011).
27. M. H. Al-Mansoori, M. A. Mahdi, and M. Premaratne, *IEEE J. Sel. Topics Quantum Electron.* **15**, 415 (2009).
28. M. N. Mohd Nasir, Z. Yusoff, M. H. Al-Mansoori, H. A. Abdul Rashid, and P. K. Choudhury, *Laser Phys. Lett.* **6**, 54 (2009).
29. J. Zhao, T. Liao, X. Yang, Z. Tong, and Y. Liu, *J. Opt.* **12**, 115202 (2010).
30. N. A. M. A. Hambali1, M. A. Mahdi, M. H. Al-Mansoori, A. F. Abas, and M. I. Saripan, *Opt. Express* **17**, 11768 (2009).